Proc. of the European Safety and Reliability Conference (ESREL 2026)
Edited by José C. Matos, Paulo B. Lourenço, Michael Beer, Daniel Oliveira,
Edoardo Patelli, Hélder S. Sousa, Rui A. Silva and Monica Santamaria
 Published by Research Publishing, Singapore.
doi: 10.3850/ESREL2026061419_esrel26-p27694-cd

Spot the Rainbow: Augmenting Global Sensitivity Methods with Graphical Visualization Techniques

Elmar Plischke
Institute of Resource Ecology, Helmholtz-Zentrum Dresden-Rossendorf, Germany. E-mail: e.plischke@hzdr.de

Mostafa Abdelhafiz
Institute of Technical Mechanics, TU Clausthal, Germany. E-mail: mostafa.abdelhafiz@tu-clausthal.de

We present three methods for visually representing sensitivity analysis results, and apply it to a radionuclide retention model in granitic host rock

Keywords: Variance-based sensitivity analysis, moment-independent importance, radioactive waste disposal

1. Introduction

Global sensitivity analysis helps the analyst to gain insight into the behavior of complex simulation models. Sensitivity analysis has the goal of identifying the ranking of the influential parameters affecting the uncertainty in the simulation results. Data-driven approaches come with a light computational burden that is mostly independent of the input dimension, so that resources can be used efficiently and data can re-analyzed using different methods. Of special interest are methods, which provide a graphical feedback of the results, as they can be used intuitively also by non-specialists.

We present the following three methods: 1) Cumulative sum of reordered normalized output (CUSUNORO) curves for visualizing first order effects, 2) Flavour method to obtain regionalized output sensitivity information using quantile-based sensitivity indices, and 3) Checkerboard partition sensitivity (indices are computed conditionally to a pair of dominant input parameters) allowing for the detection of variance-based higher order indices.

We assume that all random variables X_i, $i = 1, \ldots, d$ and Y are given on a common probability space. We denote expectation and variance by $\mathbb{E}[\cdot]$ and $\mathbb{V}[\cdot]$. In a computer simulation setting the distribution of $X = (X_1, \ldots X_d)$ is known and Y is the output of a (deterministic) simulation model $Y = g(X)$. We denote the marginal cumulative distribution function (cdf) of X_i by F_{X_i} and the output cdf by F_Y.

The application case is a geochemical simulation model for a potential radioactive waste disposal site. The Uranium sorption in a granitic rock is estimated, taking into account the interaction with the exposed surface minerals. As acidity pH and ion strength Eh are highly variable in water composition, mineral components only form minor drivers of uncertainty. Spotting their influence becomes a challenge, which we master by using the aforementioned methods.

2. The CUSUNORO curve

A look at the scatterplot between a model input parameter and a model output parameter can reveal different effects, like trends or concentrations, or demonstrate that a parameter has only an insignificant influence on the output. However, manually screening scatterplots can become tiresome business. Therefore, a technique to compress the information from a scatterplot into a curve has been suggested in [7] and is suggested as an alternative to the contribution to the sample mean plot [1]. It illustrates the deviance from the output mean, when partitioning on a sliding window of input parameters. It is called the cumulative sum of normalized reordered output (CUSUNORO) and is linked to the first order effect, which measures the degree of functional

$$\begin{aligned}\mathrm{CSN}_i(\theta) &= \frac{1}{\sqrt{\mathbb{V}[Y]}} \int_{-\infty}^{F_{X_i}^{-1}(\theta)} \mathbb{E}\left[\mathbb{E}[Y] - Y | X_i = x\right] dF_{X_i}(x) \\ &= \frac{1}{\sqrt{\mathbb{V}[Y]}} \int_0^{\theta} \mathbb{E}\left[\mathbb{E}[Y] - Y | F_{X_i}(X_i) = u\right] du = \frac{\theta}{\sqrt{\mathbb{V}[Y]}} \mathbb{E}\left[\mathbb{E}[Y] - Y | F_{X_i}(X_i) \leq \theta\right] \quad (1)\end{aligned}$$

$$\mathbb{E}\left[\int_{\mathbb{R}} (F_Y(y) - F_{Y|X_i}(y))^2 dF_Y(y)\right] = \int_0^1 \mathbb{V}[\mathbb{E}\left[\mathbf{1}\left\{Y \leq F_Y^{-1}(\alpha)\right\} \middle| X_i\right] d\alpha \quad (2)$$

dependence on single input parameters.

The CUSUNORO curve is given by (1) yielding a curve which connects $(0,0)$ with $(1,0)$ and which is invariant with respect to affine linear transformations. Here, θ codes the input quantile, so that all curves are presented in the same $[0,1]$ interval. For a sample based version with observations $(x_{j,i}, y_j)_{i=1,\ldots,d, j=1,\ldots,n}$, let π^i be the permutation that orders input X_i increasingly such that $x_{\pi^i(j),i} \leq x_{\pi^i(j+1),i}$ for $j = 1, \ldots, n-1$, and let μ_Y and σ_Y^2 be the output sample mean and variance. Then, using the reordered output

$$\mathrm{CSN}_i: \quad \theta \mapsto \frac{1}{\sqrt{n\sigma_Y^2}} \sum_{j=1}^{\lceil n\theta \rceil} \left(\mu_Y - y_{\pi^i(j)}\right) \quad (3)$$

where μ_Y and σ_Y^2 are the sample mean and empirical variance of the output Y.

The mean squared gradient of the CUSUNORO curve is an estimate of the variance-based first order effect $S_i = \frac{\mathbb{V}[\mathbb{E}[Y|X_i]]}{\mathbb{V}[Y]}$. To estimate, one can approximate the CUSUNORO curve via a polyline (with, say, 10 inner points) and then compute a gradient. For a rough lower estimate we can use the extreme points of the curve: If the CUSUNORO curve reaches an extremum at, say, $q \in [0,1]$ with value $\pm z$, then connecting this point with $(0,0)$ and $(1,0)$ leads to the lower estimate of first order effect given by $\left(\frac{1}{q} + \frac{1}{1-q}\right) z^2$. This is a good approximation if the curve is parabola-shaped. The connection of the contribution of the sample mean to the first order effects is studied in [9].

For studying higher order effects, [10] suggest the contribution to sample variance plot. We can also modify the CUSUNORO curve, considering local variance instead of local mean. For this we run the reordered output through a three-term moving variance, i. e., $y_{\pi(j)}$ is replaced by the its empirical local variance

$$\frac{1}{2}\left(y_{\pi(j-1)}^2 + y_{\pi(j)}^2 + y_{\pi(j+1)}^2\right) - \frac{3}{2}\left(\frac{1}{3}(y_{\pi(j-1)} + y_{\pi(j)} + y_{\pi(j+1)})\right)^2. \quad (4)$$

This newly generated output is then fed into (4) to obtain information on the deviation from the local variance. The mean value in this case is then $\mathbb{V}[Y](1-S_i)$ and provides an alternative estimator of first order effects.

If given multivariate output (e. g., a time series), then we can plot all CUSUNORO curves belonging to the same input into one panel. The input range can then be on the original scale instead of quantiles.

3. The Flavour Method

In some cases, one might be interested in determining which parts of the output range are affected the most by input parameters, especially when the variance-based sensitivity indices provide inconclusive results. One may consider the differences between unconditional and conditional output cdfs instead of the quadratic differences between unconditional and conditional means given the input. The sensitivity measure

$$\xi_i = \iint (F_Y(y) - F_{Y|X_i=x_i}(y))^2 dF_{X_i}(x_i) dF_Y(y) \quad (5)$$

is invariant with respect to monotonic output transformations [2]. It can be expressed as weighted quantile score. Here, [3] obtain an estimator using the relation (2). Hence, the variance

of the conditional expectation (which is the unnormalized first effect) is taken on the output quantile function. In (2), $Z^\alpha = \mathbf{1}\{Y : F_Y(Y) \leq \alpha\}$ is a binary random vector that selects all entries below the α-quantile of Y. Therefore, estimators of first order effects like CUSUNORO (as described above), EASI or COSI [6, 8] can be used to obtain this CDF sensitivity by averaging the first order effects of suitable indicator functions.

For a graphical display, we disaggregate (2) and display the map $\alpha \mapsto \mathbb{V}[\mathbb{E}[Z^\alpha|X_i]$ or $y \mapsto \mathbb{V}[\mathbb{E}\left[Z^{F_Y(y)}\middle|X_i\right]$. In [4], a link to reliability methods is established, interpreting the simulation model function $g(\cdot)$ as a limit-state function. We will therefore call these variance based sensitivity indices derived from quantile functions the reliability sensitivity. Further results in this direction are discussed by [5].

4. Checkerboard Sensitivity

In complex systems, as the number of parameters and interactions increases, estimating higher-order effects becomes significantly more challenging, especially with data-driven methods. These interactions often remain hidden when traditional sensitivity analysis methods are applied. We present a graphical method that enables visualization of third-order effects, thus providing new insights into the intricate structure of parameter interactions. We will use a first-order effect estimator on partitioned data. This partition is taken with respect to the two most important parameters identified from a first order sensitivity analysis. As we partition with respect to two parameters, the partition now presents itself as a checkerboard.

As demonstrated in Figure 1, the checkerboard method works by selecting two input parameters, then partitioning the parameter sub-space into a checkerboard grid, where each tile represents a specific combination of the selected parameters. For each tile, the first-order effect is computed based on the conditional sample of the output to variations in the inputs. These can then be displayed as a heatmap. One has the option to scale with respect to the overall output variance or the output variance with respect to the patch. The method highlights regions where parameters

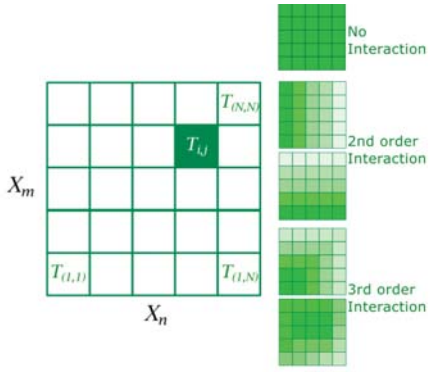

Fig. 1. Checkerboard Partitioning

exert the strongest influence, which for a deeper exploration of third-order effects and their impact on system behavior.

Fixing two input parameters i_1 and i_2 and associated partition sizes R and S the checkerboard sensitivity for $i \neq i_1, i_2$ is given by

$$S_i^{r,s} = \frac{1}{\mathbb{V}[Y]}\mathbb{V}\left[\mathbb{E}[Y|X_i]\middle| X_{i_1} \in F_{i_1}^{-1}\left(\frac{r-1}{R}, \frac{r}{R}\right], X_{i_2} \in F_{i_2}^{-1}\left(\frac{s-1}{S}, \frac{s}{S}\right]\right] \quad (6)$$

In order to have enough data available for a data-driven estimation, the sample size should satisfy $n > 64 \cdot RS$.

5. Application to a Geochemical Model

The model under investigation computes the retention of radionuclides in a granitic host rock environment. Site-specific input variables are the pH value, the redox potential Eh), the ionic strength, the total concentration of the contaminant, the total concentration of dissolved carbon dioxide, the concentration of other relevant anions and metal cations, the composition of the exposed mineral surface (which must add to 100%), and the solid-liquid-ratio which is derived from porosity. initial model simulations were performed where some of the parameters were kept constant. The model output provides the sorption coefficient Kd for the uranium species. A total of 14032 simulations is available, with 13 uncertain input parameters in

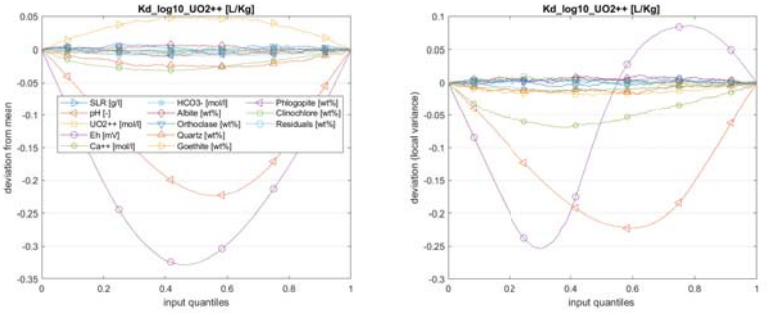

Fig. 2. Cumulative sum of reordered normalized output curves for the Radionuclide Retention model.

the model. Figure 2 shows the CUSUNORO plots for deviations from the mean (left panel) and deviations from the variance (right panel). We see that the first order effects are dominated by two parameters, Eh and pH, followed by Goethite, Calcium and Quartz. We can use the extreme values and positions of the CUSUNORO curves to derive lower bounds for first order effects: $S(Eh) > (-0.33)^2(\frac{1}{0.47} + \frac{1}{1-0.47}) \approx 0.44$ and $S(pH) > (-0.22)^2(\frac{1}{0.54} + \frac{1}{1-0.54}) \approx 0.19$. The sensitivity of Goethite is then $S(Goethite) > 0.05^2(\frac{1}{0.5} + \frac{1}{0.5}) = 0.01$, and we observe a clear decrease in the sensitivities. For the deviation from the variance, note that the curve for Eh changes signs, so that we expect to find a scatterplot of Eh versus the output that offers large changes in the local variance. This can be seen in Figure 3 where the scatterplots for the two most significant parameters are displayed. We observe that no clear trend, separating a signal and an error term, is possible, which makes this example hard to handle with first-order effects. The change in the local variance is due to interactions in the model. We will try to spot possible interactions with a checkerboard sensitivity analysis.

But first, we consider a moment-independent sensitivity analysis to obtain regionalized information when a parameter is active. The results from a cdf-based approach can be found in Fig. 4. We use a logarithmic scale to obtain information from the minor contribution input parameters. We observe that the Calcium ion concentration influences the low Kd range, while Goethite and Quartz are responsible for effects in the larger Kd values. Strongly regionalized sensitivity information is again a sign of the presence of interaction effects. However, no clear picture emerges which possible parameter combinations lead to these effects. Here, Goethite, Quartz and Albite all show their maximum in the same output range. The overall dominance of pH and Eh is also visible here.

To obtain a different viewpoint, we switch to checkerboard sensitivity, as demonstrated in Figure 5. Each pixel represents a first order effect conditionally on a partition of the two most important input parameters, Eh and pH. As these two parameters are also included, and still show effects, the partition is too coarse to resolve all details. Nevertheless, we observe Ca^{++} to be active between pH 7.0 and 8.5 and for Eh larger than -300 mV. Being dependent on both parameters is then a sign of third order interaction. The physical explanation for this behavior is the solubility limit of carbonates. To a lesser extent, we observe the same behavior with $UO_2{}^{++}$ that is only active for Eh$>$ 0 and pH$<$ 7. The influence of other parameters is barely visible on this scale. Also, SLR shows visually no effects at all, so that its parameter value might be fixed at a constant value, and it could be removed from the random parameter set, decreasing the overall model dimensionality.

6. Discussion

Uncertainty quantification and sensitivity analyses, which are carried out in the context of the safety assessment or performance assessment of a radioactive waste repository, assist in building a

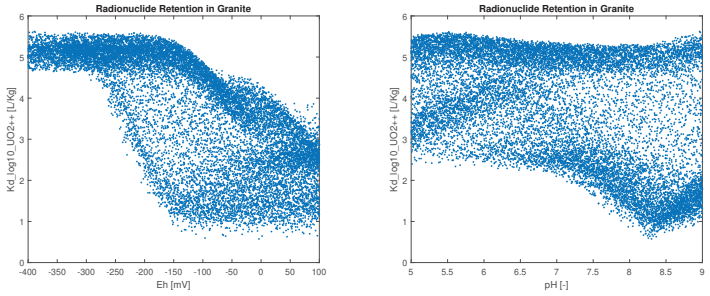

Fig. 3. Scatterplots for the most important input parameters, Eh and pH, in the Radionuclide Retention model.

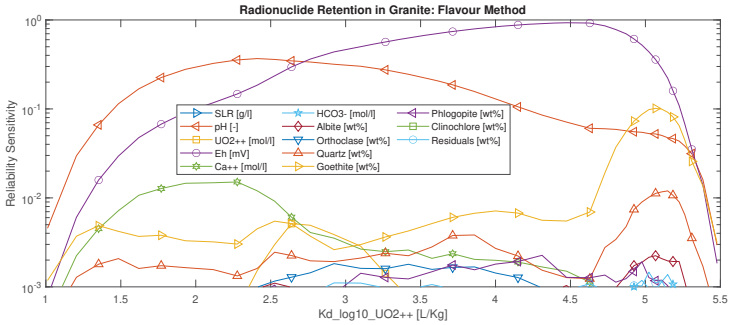

Fig. 4. Regionalized sensitivity information from a cdf-based approach for the Radionuclide Retention model.

better understanding of the system relationships, optimizing resources, and gaining confidence in the performance of the system and in meeting certain set requirements (e. g., compliance demonstrations). Especially in safety-critical applications, simulation models should be as robust as possible to defend them against regulatory and public inquiries.

In our context, the observations made by the graphical sensitivity analysis help in building confidence in the simulation code: Are the observed effects linked to physical effects and can they be explained, or is the code and the relevant databases to be assessed for consistency? As such, these graphical tools serve as a tool to bring the sensitivity analyst and the model builder together to discuss and improve the model understanding.

One can also envision that these visualizations allow for a broader use, enabling communication with non-specialists.

Data and Code Availability

The dataset is available upon request. MATLAB scripts for performing sensitivity analysis are available from `https://gitlab.gwdg.de/elmar.plischke/global-sensitivity-analysis-collection`. A Python software platform that implements the methods used is available from `https://gitlab.gwdg.de/mostafa.abdelhafiz/sa-toolbox`.

Acknowledgments

This work is funded by the German Federal Ministry for Environment, Climate Action, Nature Conservation and Nuclear Safety (BMUKN) under grant #02E12112A (SANGUR). The authors thank Alexandra Duckstein, Solveig Pospich and Vinzenz Brendler (HZDR) for providing the simulation data and discussing results.

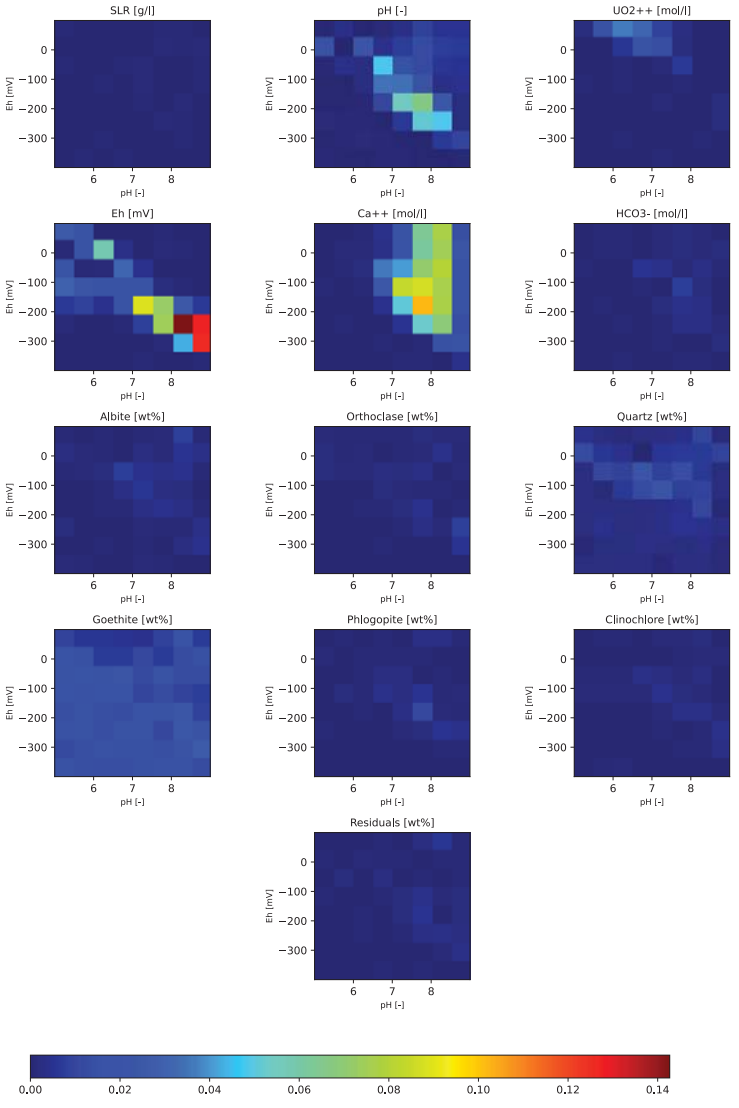

Fig. 5. Checkerboard partitioning on pH (x-axis) and Eh (y-axis).

References

1. R. Bolado-Lavin, W. Castaings, and S. Tarantola. Contribution to the sample mean plot for graphical and numerical sensitivity analysis. *Reliability Engineering&System Safety*, 94(6):1041–1049, 2009.
2. E. Borgonovo, S. Tarantola, E. Plischke, and M. D. Morris. Transformations and invariance in the sensitivity analysis of computer experiments. *Journal of the Royal Statistical Society, Series B*, 76:925–947, 2014.
3. F. Gamboa, T. Klein, and A. Lagnoux. Sensitivity analysis based on Cramér–von Mises distance. *SIAM/ASA J. Uncertainty Quantifi-*

cation, 6(2):522–548, 2018.

4. L. Li, Z. Lu, J. Feng, and B. Wang. Moment-independent importance measure of basic variable and its state dependent parameter solution. *Structural Safety*, 38:40–47, 2012.
5. I. Papaioannou and D. Straub. Variance-based reliability sensitivity analysis and the FORM α-factors. *Reliability Engineering&System Safety*, 210:#107496, 2021.
6. E. Plischke. An effective algorithm for computing global sensitivity indices (EASI). *Reliability Engineering&System Safety*, 95(4):354–360, 2010.
7. E. Plischke. An adaptive correlation ratio method using the cumulative sum of the reordered output. *Reliability Engineering&System Safety*, 107:149–156, 2012.
8. E. Plischke. How to compute variance-based sensitivity indicators with your spreadsheet software. *Environmental Modelling&Software*, 35:188–191, 2012.
9. N. Saint-Geours, S. Tarantola, V. Kopustinskas, and R. Bolado-Lavin. Computing first-order sensitivity indices with contribution to the sample mean plot. *Journal of Statistical Computation and Simulation*, 85(7):1334–1357, 2015.
10. S. Tarantola, V. Kopustinskas, R. Bolado-Lavin, A. Kaliatka, E. Uškuras, and M. Vaišnoras. Sensitivity analysis using contribution to sample variance plot: application to a water hammer model. *Reliability Engineering&System Safety*, 99:62–73, 2012.